Journal of Power Sources 250 (2014) 266–273

Contents lists available at ScienceDirect

Journal of Power Sources

journal homepage: www.elsevier.com/locate/jpowsour

Water transport characteristics of the passive direct formic acid fuel cell

Takuya Tsujiguchi*, Takanori Iwakami, Soshi Hirano, Nobuyoshi Nakagawa

Department of Chemical and Environmental Engineering, Graduate School of Engineering, Gunma University, 1-5-1 Tenjincho, Kiryu, Gunma, Japan

HIGHLIGHTS

- The water transport characteristics of the DFAFC were investigated.
- The water flux of DFAFC increased with the increasing current density.
- The water flux of DFAFC decreased with the decreasing membrane thickness.
- The water transport characteristics of the DFAFC differed from those of DMFC.

ARTICLE INFO

Article history:
Received 7 September 2013
Received in revised form
18 October 2013
Accepted 22 October 2013
Available online 8 November 2013

Keywords:
Direct formic acid fuel cell
Water transport
Passive operation
Nafion membrane
Hydrophobic filter

ABSTRACT

The water transport characteristics of the passive DFAFC were investigated to obtain a general understanding of the water transport characteristics through the membrane in the DFAFC in this study. Effects of the current density, membrane thickness and formic acid concentration on the water flux thorough the membrane in the passive DFAFC were investigated and they were compared with those of the DMFC and the PEFC. It was found that the water crossover through the membrane of the passive DFAFC linearly increased with increasing current density irrespective of the membrane thickness similar to the DMFC; however, the water flux was smaller than that of the DMFC. Referring to the effect of the membrane thickness on the water flux, the water flux from the anode to the cathode increased with increasing the membrane thickness in the DFAFC, although it decreased with increasing membrane thickness in the DMFC. Moreover, the water flux increased with decreasing fuel concentration in the DFAFC, although the water crossover in the DMFC was not influenced by the fuel concentration. From these results, it was found that the water transport characteristics in the DFAFC were different from those in the DMFC.

1. Introduction

Direct formic acid fuel cells, DFAFCs, have received considerable attention as an alternative power source for electric portable devices due to their high power density which is comparable to that of the PEMFC, polymer electrolyte fuel cell operated with hydrogen–oxygen, and 6 times that of direct methanol fuel cells, DMFCs [1–3]. Moreover, it is broadly known that the fuel crossover rate in the DFAFC is lower than that in the DMFC [4–7]. On the other hand, the water transport characteristics which are a key factor in stable and efficient operation of a fuel cell using a polymer electrolyte membrane in the DFAFC have not been revealed.

It has been recognized that water management is a critical issue for the performance and durability of a fuel cell employing the polymer electrolyte membrane because sufficient water content is necessary to maintain the high proton conductivity of the membrane. On the other hand, excessive liquid water can block the pores of the catalyst and gas diffusion layer and may cause flooding. Typically, the water management in a PEMFC stands for a balance of water in between membrane hydration and cathode flooding [8,9]. However, the problem is more challenging for a DMFC. Water management in a DMFC refers to providing water for the anode, while preventing cathode flooding. Unlike the hydrogen fuel cells, membrane hydration is not an important issue in DMFCs as long as water is provided from the methanol solution [10]. Especially, when the DMFC is operated in a passive mode which does not use a pump and/or blower for supplying a fuel and oxygen, the water management becomes more serious because the liquid water, which is produced by the cathode reaction and methanol oxidation reaction due to the methanol crossover at the cathode, is likely to

* Corresponding author. Present address: School of Mechanical Engineering, College of Science and Engineering, Kanazawa University, Kakumamachi, Kanazawa, Ishikawa, Japan. Tel.: +81 762646473; fax: +81 762646497.
E-mail address: tsujiguchi@se.kanazawa-u.ac.jp (T. Tsujiguchi).

0378-7753/$ – see front matter © 2013 Elsevier B.V. All rights reserved.
http://dx.doi.org/10.1016/j.jpowsour.2013.10.094

accumulate in the cathode. Therefore, numerous studies of the water transport characteristics in the PEMFC [11–13] and DMFC [14–16] have been carried out. On the other hand, to the best of our knowledge, there have been no reports about the water transport characteristics in the DFAFC. Because the DFAFC does not use water for the anode reaction and the high concentration of formic acid shows a hygroscopic property [17], the water transport characteristics are likely to differ from those in the DMFC. Of course, the water transport characteristics in the DFAFC are also likely to differ from those of the PEMFC because the DFAFC uses a liquid fuel for the anode. Therefore, it is necessary to investigate the water transport characteristics in the DFAFC and compare them to those of the DMFC and PEFC.

This work aims to achieve a general understanding of the water transport characteristics through the membrane in the DFAFC. The passive DFAFC with the insertion of a hydrophobic filter (HF) at the cathode surface was used in this study for two reasons. First, the passive DFAFC was suffered from serious flooding [18] so that the investigation of the water transport characteristics of the passive DFAFC is more important than those of the active DFAFC. Second, we demonstrated that the flooding could be improved and the current density was increased by inserting the hydrophobic filter at the cathode surface in our previous study [18]. From this result, the HF enables measuring the water crossover (WCO) of the passive DFAFC over a wide range of current density. Using this structure, the effects of the membrane thickness, formic acid concentration and current density on the WCO were investigated by measuring the WCO during a 2 h operation. Two different operations were conducted to measure the water crossover in the wide range of current density: the 2 h power generations at a different constant voltage with and without HF and the 2 h operations at the same constant voltage using a different HF containing different amounts of fluorinated ethylene propylene copolymer (FEP). Finally, the water transport characteristics were compared with those of the DMFC and the PEMFC to characterize the water transport characteristics of the passive DFAFC.

2. Experimental

2.1. Membrane electrode assembly (MEA) preparation

NR 212, Nafion 115 and Nafion 117 (Dupont) were used as the polymer electrolyte membrane. In order to activate the proton conductivity, the membranes were pretreated by sequential immersion in boiling solutions of 3 vol-% H_2O_2 for 1 h, de-ionized water for 1 h, 0.5 mol l^{-1} H_2SO_4 for 1 h, and de-ionized water for 1 h, in that order. Palladium black (Alfa Aesar) and platinum black (HiSPEC 1000, Johnson Matthey Fuel Cells Co., Ltd.) were used as the catalysts for the anode and the cathode, respectively. The catalyst inks were prepared by dispersing an appropriate amount of the catalyst in a solution of de-ionized water, isopropyl alcohol, and 5 wt% Nafion solution (Wako Pure Chemical Industries, Ltd.). For the anode, the Pd ink was coated on the microporous layer, which was prepared with 1 mg cm^{-2} of a carbon black containing 10 wt% Nafion on the carbon cloth (35% Teflonized, ElectroChem, Inc.) to form the electrode. For the cathode, the Pt ink was coated on the carbon paper (35% Teflonized, ElectroChem, Inc.) with a microporous layer in a similar manner. The catalyst loadings were 6 mg cm^{-2} for Pd, the anode, and Pt, the cathode, respectively. The ionomer loadings of the catalyst layer were 15 wt% for the anode and 10 wt% for the cathode. The MEA was then fabricated by sandwiching the membrane between the anode and the cathode and hot pressing them at 408 K and 5 MPa for 3 min. The projected area of the electrode was 4.84 cm^2 (2.20 × 2.20 cm).

2.2. Cell structure and hydrophobic filter

Fig. 1 shows a schematic diagram of the passive DFAFC cell used in this study. A fuel reservoir, 12 cm^3 in capacity, was prepared in the anode compartment. The MEA was sandwiched between the two current collectors, which were plates of stainless steel, 1 mm, coated with gold, having open holes, and a 74% open ratio.

In some operations, the hydrophobic filter, HF, 5, was inserted between the cathode and the cathode current collector. The HFs which have different hydrophobicity were prepared by coating a carbon black layer, 1 mg cm^{-2} carbon black on the carbon paper (35% Teflonized, ElectroChem, Inc.) with FEP, fluorinated ethylene propylene copolymer, and heating them to 100 °C for 1 h. The FEP coating was repeated several times until the FEP content reached a certain weight. Table 1 shows the loading of the FEP and the contact angle of the HF. The contact angle was measured by a contact angle meter (CA-X, Kyowa Interface Science Co., Ltd.), and the hydrophobicity increased with the increasing FEP loadings. The projected area of the filter was 4.84 cm^2 which was the same as that of the electrodes.

2.3. Measurement of the power generation characteristics

The DFAFC was operated in a complete passive mode, i.e., the cathode was air breathing and the fuel was supplied from the tank to the anode electrode without a pump. All experiments were conducted under the room conditions, 1 atm, 293–298 K. A formic acid solution was prepared by diluting formic acid (special grade reagent, Wako Pure Chemical Industries, Ltd.) with distilled water (Kyoei Pharmaceutical Co., Ltd.). The current versus time, i–t, characteristics were also measured at different cell voltages, 0.3 V, 0.4 V and 0.5 V. All the electrochemical measurements were conducted using an electrochemical measurement system (Hz-5000, Hokuto Denko, Co., Ltd.). The entire cell weight and the concentration of the solution were also measured at the beginning and the end of the i–t measurements to calculate the formic acid and water crossovers using the precision balance (GF-600, A&D Company, Limited). When the cell weight was measured after the i–t operation, water droplets were removed from the cathode surface to obtain an accurate weight loss of the fuel since the accumulated water droplet likely causes an overestimation of the final cell weight. The formic acid concentration was measured by gas chromatography equipped with a TCD detector and a Porapak T column (Shimadzu, GC14-B).

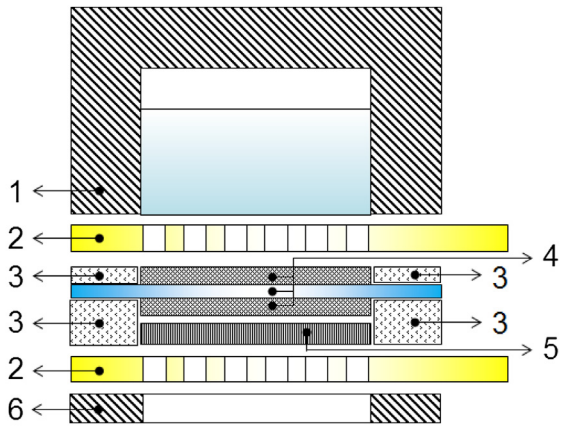

Fig. 1. Schematic diagram of the passive DFAFC cell.

Table 1
Loadings of the FEP and the contact angle of the HFs.

Sample	Loadings of the FEP	Contact angle [°]
HF-1.1	1.1 mg cm^{-2}	148.0
HF-0.5	0.5 mg cm^{-2}	138.6
HF-0	0 mg cm^{-2}	135.2

Because the anode performance degraded with the operation due to the catalyst poisoning, the following regeneration process, RP, was conducted. After power generation, the formic acid solution was replaced with fresh water and the cell was swung to wash the anode surface. This washing was repeated until the residual cell voltage decreased to 0.1 V according to the previous report by Zhou et al. [19]. The anode performance was completely regenerated by this RP process to the initial condition.

2.4. Calculation of the formic acid and water fluxes

The average flux for each of the formic acid and water across the MEA during the i–t measurement was calculated based on weight loss and a decrease in the formic acid concentration of the solution. The weight loss, ΔW, which was obtained by subtracting the final weight of the remaining solution in the reservoir at the end of the i–t measurement, W_e, from that of the initial weight, W_i, can be expressed as follows:

$$\Delta W = W_i - W_e = \Delta W_{cf} + \Delta W_{cw} + \Delta W_{rf} + \Delta W_{ef} + \Delta W_{ew} \quad (1)$$

where ΔW_{cf} and ΔW_{cw} are the weight losses of the formic acid and that of water due to the crossover from the anode to the cathode, respectively. The ΔW_{rf} is the weight loss of the formic acid consumed by the anode reaction, and this was calculated by integrating the area of the i–t curve assuming the complete oxidation of formic acid:

$$HCOOH \rightarrow 2H^+ + CO_2 + 2e^- \quad (2)$$

as follows:

$$\Delta W_{rf} = \frac{M_f A \int_0^t i(t)dt}{2F} \quad (3)$$

where M_f is the molecular weight of the formic acid, A is the apparent electrode area, t is the time of the i–t measurement and F is Faraday's constant. ΔW_{ef} and ΔW_{ew} are the weight loss due to the evaporation of the solution and CO_2 gas exhaust through the injection tube open to the environment. However, it was experimentally confirmed that they were less than 1% of weight loss of the solution during the i–t measurement, therefore they were negligible. ΔW_{cf} and ΔW_{cw} can be expressed as follows:

$$\Delta W_{cf} = (W_i\omega_i - W_e\omega_e) - \Delta W_{rf} \quad (4)$$

$$\Delta W_{cw} = \Delta W - (W_i\omega_i - W_e\omega_e) \quad (5)$$

where ω_i and ω_e are the mass concentration of the formic acid solution in the reservoir at the beginning of the i–t measurement and the end of the i–t measurement, respectively. Hence, the crossover flux of the formic acid, J_f, and that of the water, J_w, were calculated as

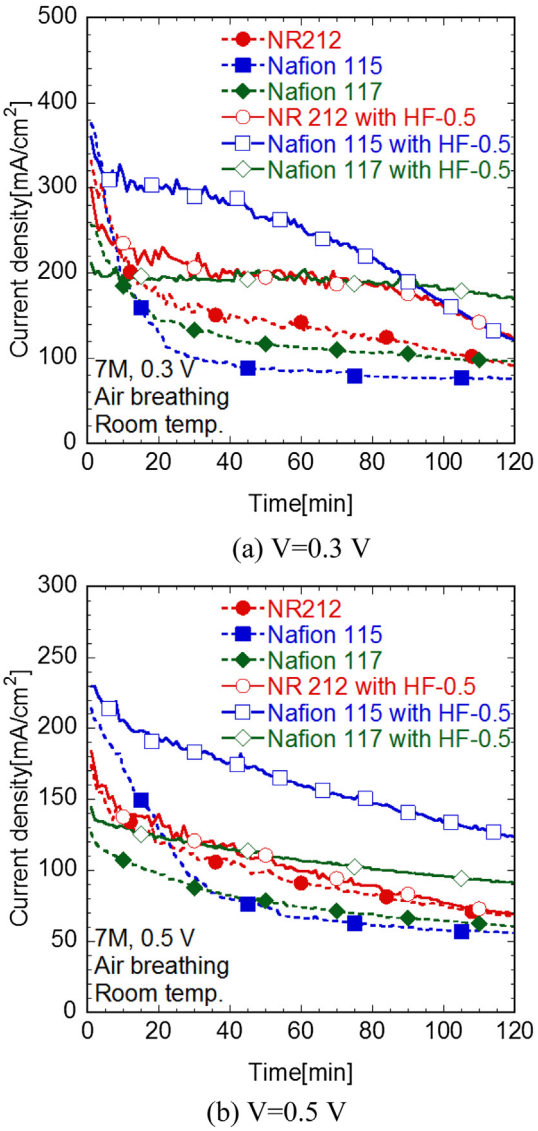

Fig. 2. Effect of the membrane thickness on the current density profiles in the operation at constant voltage, 0.3 V or 0.5 V, using different membranes.

$$J_f = \frac{\Delta W_{cf}}{At} \quad (6)$$

$$J_w = \frac{\Delta W_{cw}}{At} \quad (7)$$

In this study, the formic acid and the water transports through the membrane were considered to be governed by the three transport mechanisms similar to those in the DMFC: i.e., electro-osmotic drag, diffusion and convection. Hence, the formic acid and the water flux were expressed as follows:

$$J_f = J_{feo} + J_{fdiff} + J_{fc} \quad (8)$$

$$J_w = J_{weo} + J_{wdiff} + J_{wc} \quad (9)$$

where J_{feo} and J_{weo} represent the formic acid and water flux by electro-osmotic drag, J_{fdiff} and J_{wdiff} represent the formic acid and water flux by diffusion and J_{fc} and J_{wc} represent the formic acid and water flux by convection, respectively. Note that the positive flux

means the flux from the anode to the cathode and the negative flux means the flux from the cathode to the anode.

3. Result and discussion

3.1. Effect of the membrane thickness on the current profiles and formic acid/water flux through the membrane

Fig. 2 shows the effect of the membrane thickness on the current density profiles in the operation at constant voltage, 0.3 V and 0.5 V, using HF-0.5. Except for the case of NR 212 operated at 0.5 V, the performance degradation could be drastically improved by inserting the HF similar to our previous report [18]. Fig. 3 shows the effect of the average current density and membrane thickness on the formic acid and water flux through the membrane during the i–t measurements shown in Fig. 2. The formic acid flux reasonably decreased with the increasing membrane thickness; 0.0037 mol m^{-2} s^{-1} of formic acid flux was obtained at 100 mA cm^{-2} when Nafion 115 was used. Jeong et al. reported that the formic acid crossover current of a DFAFC equipped with Nafion 115 at current density of 100 mA cm^{-2} when 6 M formic acid was used was 70 mA cm^{-2} which was equivalent to 0.0036 mol m^{-2} s^{-1} [7]. Although the formic acid concentration in this work was slightly different from their report, the formic acid flux obtained in this study agreed with their study. In the case of NR 212, the formic acid flux was highest in the three membranes, suggesting that the performance degradation which occurred with NR 212 was mainly caused by the formic acid crossover. Therefore, the performance was not improved by inserting the HF because the HF can only improve the performance degradation duet to the flooding.

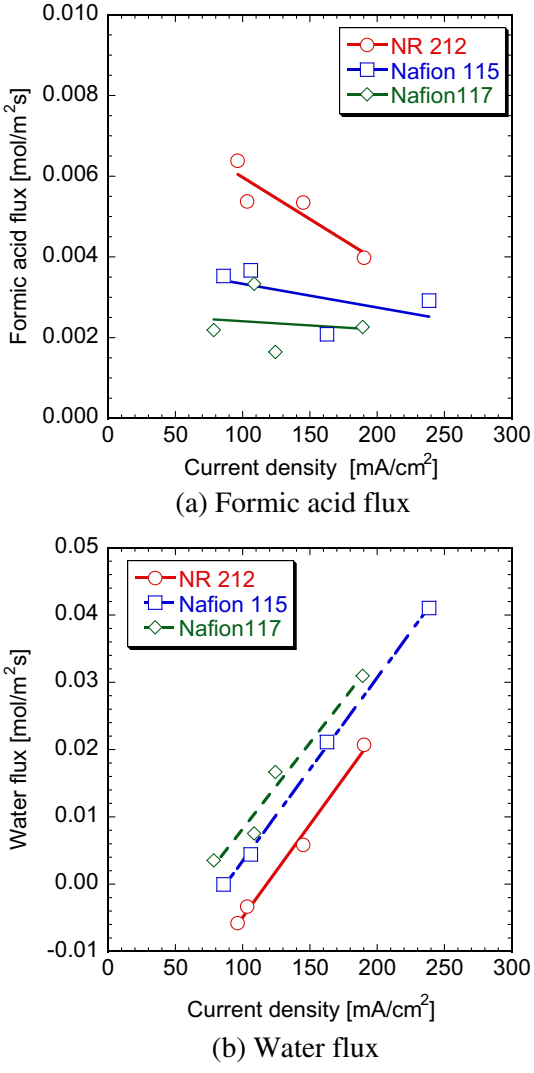

Fig. 3. Effect of the average current density and membrane thickness on the formic acid and the water flux during the i–t measurement shown in Fig. 2.

The water flux linearly increased with the increasing average current density irrespective of the membrane. The slopes of the line were nearly similar for each membrane; however, the water flux increased with the increasing membrane thickness. Especially, in the case of NR 212, the water flux showed a negative value under 120 mA cm^{-2}. A negative flux means that the water was transported from the cathode to the anode. Based on Eq. (9), the water flux was expressed by the sum of the flux by electro-osmotic drag, diffusion and convection; therefore, the water flux by diffusion and/or convection should be a negative value because the water flux by electro-osmotic drag should be a positive value. From this point, it was considered that the water flux by diffusion and/or convection from the cathode to the anode increased with the decreasing membrane thickness, resulting in a decrease in the total water flux with increasing membrane thickness.

3.2. Effect of the formic acid concentration on the formic acid and water crossover

3.2.1. Current density profiles for the DFAFC with the different HFs

Fig. 4 shows the effect of the FEP content of the HF on the current density at a constant voltage operation of 0.4 V using different membranes. 5 M and 10 M formic acid were used in the case of NR 212 and Nafion 117, respectively. In the case of NR 212 as shown in Fig. 4(a), the drastic drop in the current density within 20 min could be improved by the HF, and the current density after 20 min increased with the increasing FEP content of the HF because an increase in the FEP content, i.e., the hydrophobicity of the HF, promoted the exhaust of the water from the cathode surface to the air. Based on these results, it was suggested that the current density of the passive DFAFC was restricted by the drainability of the cathode surface, because the drainability must be improved by an increase in the hydrophobicity of the HF. On the other hand, the current densities gradually decreased with time after 20 min irrespective of the FEP content. This was due to anode poisoning [17,19] and/or a decrease in the formic acid concentration. Similar to the case of NR 212, the current density after 20 min increased with the increasing FEP content of the HF in the case of Nafion 117 as shown in Fig. 4(b). However, the degree of the performance improvement due to the increase in FEP content was smaller than that for NR 212. This was due to the high formic acid crossover by using a high concentration of formic acid. In other words, the performance was not restricted by the flooding in this case. This was the reason why the degree of the performance improvement of Nafion 117 which used 10 M formic acid was lower than that of NR 212 which used 5 M formic acid.

3.2.2. Effect of the formic acid concentration on the formic acid and water crossover

The effect of the formic acid concentration and average current density on the formic acid and water flux, calculated for the data shown in Fig. 4, is shown in Figs. 5 and 6. Irrespective of the membrane thickness, the formic acid fluxes reasonably increased with the increasing formic acid concentration due to the increase in the concentration gradient of formic acid from the anode to the cathode. On the other hand, the water fluxes decreased with the increasing

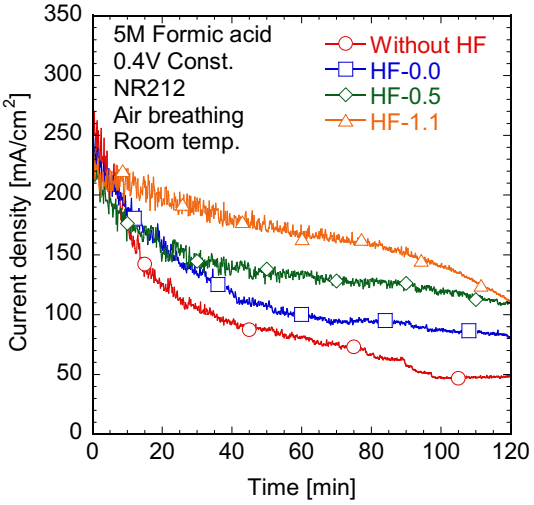

(a) NR 212 using 5M formic acid

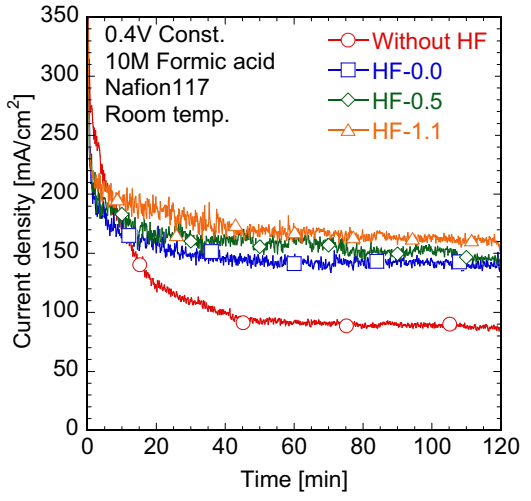

(b) Nafion 117 using 10 M formic acid

Fig. 4. Effect of the FEP content of the HF on the current density profiles under the constant voltage operation at 0.4 V using different membranes.

formic acid concentration irrespective of the membrane thickness. This would be caused by the increase in the water flux from the cathode to the anode by diffusion. Therefore, because the use of high concentration formic acid promoted the increase in the water flux by diffusion from the cathode to the anode which results in a decrease in the total water flux from the anode to the cathode, the flooding could be reduced by using a high concentration of formic acid.

3.3. Comparison of the water transport characteristics in the different fuel cells; DFAFC, PEMFC and DMFC

In order to characterize the water transport in the DFAFC, the effect of the current density, membrane thickness and fuel concentration on the water flux in the DFAFC was compared with those of DMFC and PEFC. Table 2 shows the operation and calculation conditions in the reference paper and this study. The DMFC operated in a passive mode [20], semi-passive mode [21], active mode [22–24] and a typical PEFC operated at high temperature [25] and an air breathing PEFC operated at low temperature [26] were selected as a reference. Because some reports indicated only the net water transport coefficient, α, the water flux was estimated using the following equations by authors:

$$\alpha = \frac{J_w}{I}F \tag{10}$$

where F is the Faraday constant and I is the current density.

3.3.1. Comparison of the relationship between water transport and the current density in different fuel cells

Fig. 7 shows the comparison of the water flux in the DMFC, PEFC and DFAFC employing Nafion 115. The water fluxes linearly increased with increasing current density irrespective of the type of fuel cell, hence, the slopes and the y-intercept of the line shown in Fig. 7 are summarized in Table 3. The water flux was expressed as the sum of the water flux by electro-osmotic drag, J_{weo}, diffusion, J_{wdiff}, and convection, J_{wc}, as shown in Eq. (9), and these could be expressed by referring to the water transport in the DMFC [23] as follows:

$$J_{weo} = \kappa\frac{i}{F} \tag{10}$$

$$J_{wdiff} = D_{eff}\frac{c_{la} - c_{lc}}{\delta_m} \tag{11}$$

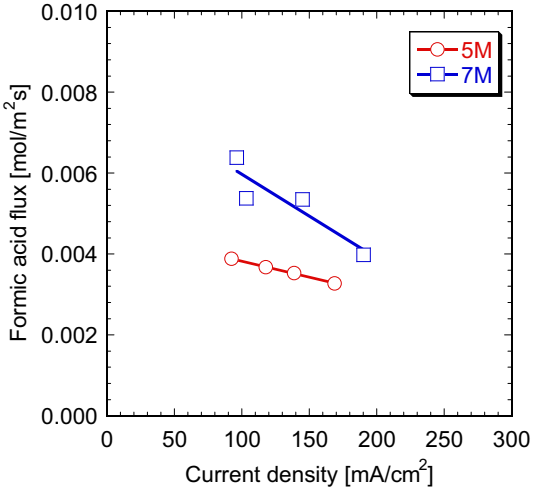

(a) Formic acid flux

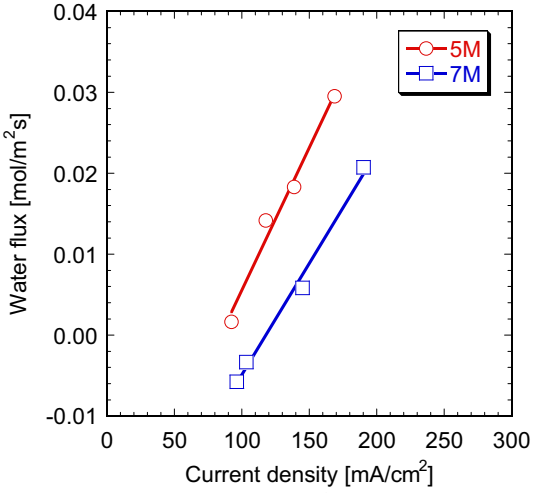

(b) Water flux

Fig. 5. Effect of the formic acid concentration and average current density on the formic acid and water flux when NR 212 was used. The fluxes at 5 M were obtained during the i–t measurements shown in Fig. 4(a). The fluxes at 7 M shown in Fig. 3 were replotted.

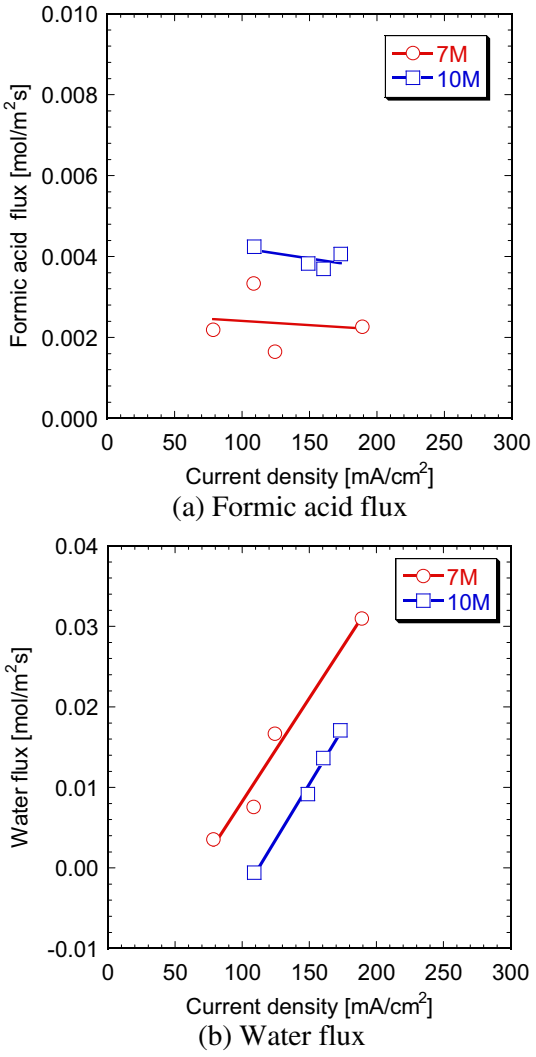

Fig. 6. Effect of the formic acid concentration and average current density on the formic acid and water flux when Nafion 117 was used. The fluxes at 10 M were obtained during the i–t measurements shown in Fig. 4(b). The fluxes at 7 M shown in Fig. 3 were replotted.

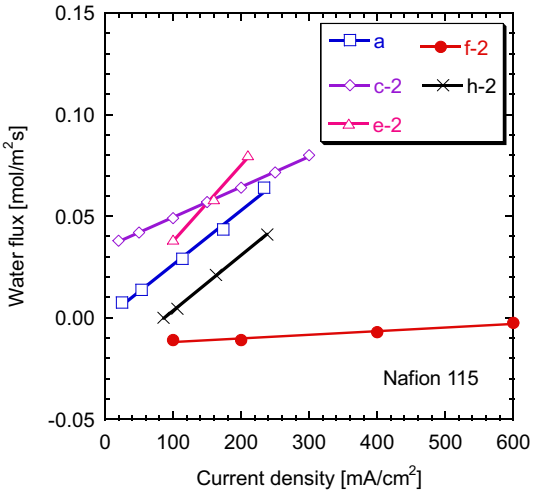

Fig. 7. Comparison of the water flux among different types of fuel cells employing the Nafion 115.

$$J_{wc} = \frac{K\rho(p_{la} - p_{lc})}{\mu M_w \delta_m} \quad (12)$$

where κ is the electro-osmotic drag coefficient in the membrane, D_{eff} is the effective diffusivity of water in the membrane, δ_m is the membrane thickness, c_{la} and c_{lc} are, respectively, liquid water concentrations at the anode and cathode surfaces of the membrane, K is the permeability through the membrane, ρ is the density of water, μ is the viscosity of liquid water, M_w is the molecular weight of water, and p_{la} and p_{lc} are, respectively, liquid water pressure at the anode and cathode surfaces of the membrane. From these equations, it was found that the slope of the line, shown in Fig. 7 and Table 3, means the increment in the water flux due to the increase in the current density, mainly J_{weo}, and the y-intercepts of the line means the water flux of $J_{wdiff} + J_{wc}$ because J_{weo} is zero at 0 mA cm^{-2}. Based on these aspects, it was found that the slope of the DFAFC, h-2, was similar to that of the DMFC, a, c-2 and e-2 from Table 3. This result suggested that the increment in the water flux due to the increase in current density in the DFAFC was similar to that in the DMFC. In the DMFC, not only an increase in J_{weo} but also in $J_{wdiff} + J_{wc}$ due to the increase in the water content at the cathode

Table 2
Operation and calculation conditions in the reference paper and this study.

	Type	Anode condition	Cathode condition	Temperature	Membrane	Remarks	Reference
a	DMFC	3 M, passive	Air breathing	22–24 °C[a]	Naf 115	Experiment	[20]
b	DMFC	4 M, 1.0 ml min^{-1}	Air breathing	25 °C[a]	Naf 117	Calculation	[21]
c-1	DMFC	1 M[b]	Air flow[b]	70 °C	Naf 112	Calculation	[22]
c-2					Naf 115		
c-3					Naf 117		
d-1	DMFC	2 M, 2 ml min^{-1}	O_2, 300 sccm	70 °C	Naf 112	Experiment	[23]
d-3					Naf 117		
e-1	DMFC	1 M, Stoichi 3	Air, Stoichi 3	70 °C	Naf 112	Experiment	[24]
e-2					Naf 115		
e-3					Naf 117		
f-1	PEFC	H_2, RH 40%, Stoichi 2	Air, RH = 100%, Stoichi 3	70 °C	Naf 112	Experiment	[25]
f-2					Naf 115		
f-3					Naf 117		
g	PEFC	H_2, dry, Stoichi 5	Air breathing	35 °C	NRE-211	Experiment	[26]
h-1	DFAFC	7 M, passive	Air breathing	25 °C[a]	NR 212	Experiment	This study Fig. 3(b)
h-2					Naf 115		
h-3					Naf 117		

[a] Surrounding air temperature.
[b] Flow rate was not indicated.

Table 3
Slopes and intercepts of the line indicated in Fig. 7.

	Type	Slope ($\times 10^4$)	Intercept ($\times 10^2$)
a	DMFC	2.67	−0.04
c-2	DMFC	1.49	3.45
e-2	DMFC	3.75	0.008
f-2	PEFC	0.18	−1.37
h-2	DFAFC	2.72	−2.38

and the decrease in the water content at the anode with increasing current density was reported [22,23]. Based on the fact that the slope of the line for the DFAFC was similar to that of the DMFC, the variation in the water flux with current density in the DFAFC would be similar to that of the DMFC as mentioned above. On the other hand, the *y*-intercepts of the DFAFC and PEFC showed a negative value and these differed from that of DMFC, which is almost zero or a positive value. Considering the fact that the J_{wc} is nearly zero at 0 mA cm^{-2} because the p_{la} and p_{lc} were almost equal, the J_{diff} for DFAFC and PEFC showed a negative value at 0 mA cm^{-2}. In the PEFC referred to in this study, the relative humidity of the anode gas was 40% and that of the cathode gas was 100%; therefore, it can be understood that the water was easily transported from the cathode to the anode [25]. Contrary to this, in the case of the DFAFC, the water would be transported from the cathode to the anode by the hygroscopic property of the formic acid [17,27]. From these results, it was found that the water transport behavior of the DFAFC under open circuit condition greatly differed from that of the DMFC, although liquid fuels are used in both types of fuel cells.

3.3.2. Comparison of effect of the membrane thickness on the water transport characteristics in the different fuel cells

Fig. 8 shows the effect of the membrane thickness and the current density on the water flux in different fuel cells, and Table 4 shows the slopes and the *y*-intercepts of the lines shown in Fig. 8. Except for the water flux of d-3 shown in Fig. 8(b), the water flux was linearly increased or decreased with the current density. Because the water flux of d-3 did not show the linear dependency on current density, the slope is not indicated and the *y*-intercept is parenthesized in Table 4(b). Irrespective of the membrane thickness, the slope of the DFAFC was similar to that for the DMFC except for d-1, and the *y*-intercept of the DFAFC was lowest among the three types of fuel cell. Although the water flux of the PEFC, g, and DMFC, b, operated in the air breathing mode were also shown in Table 3, the *y*-intercept of the DFAFC is lowest among the three types of fuel cells. This result suggested that the negatively large value of the *y*-intercept in the DFAFC was not caused by the air breathing operation, but by the use of formic acid. Referring to the effect of the membrane thickness on the slopes and intercepts, the slopes were not influenced by the membrane thickness irrespective of the type of fuel cell, while different behavior was observed in the intercepts. In the DMFC, the intercepts decreased or were nearly constant with the increasing membrane thickness, while the intercepts of DFAFC and PEFC increased with the increasing membrane thickness. This difference could be caused by the direction of the J_{wdiff}. The absolute value of J_{wdiff} decreased with increasing membrane thickness based on Eq. (11); hence, the J_w of DMFC decreased with increasing membrane thickness. On the other hand, in the case of the DFAFC and PEFC, because the J_{wdiff} showed a negative value, the decrease in the absolute value of J_{wdiff} caused a positive increase in J_w, and the J_w of the PEFC and DFAFC increased with increasing membrane thickness as shown in Fig. 8. This water transport behavior was quite characteristic of the DFAFC, which was opposite to that of the DMFC, when the membrane thickness was varied. From these results, it was suggested that the flooding caused by a water crossover can be reduced by using a thinner membrane in the DFAFC.

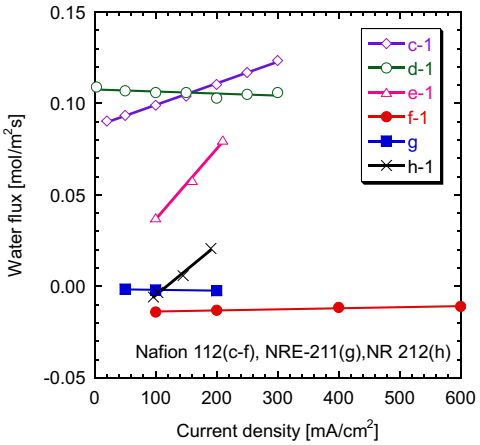

(a) Nafion112 (c-1, d-1, e-1, f-1), NRE 211 (g) and NR 212(h-1)

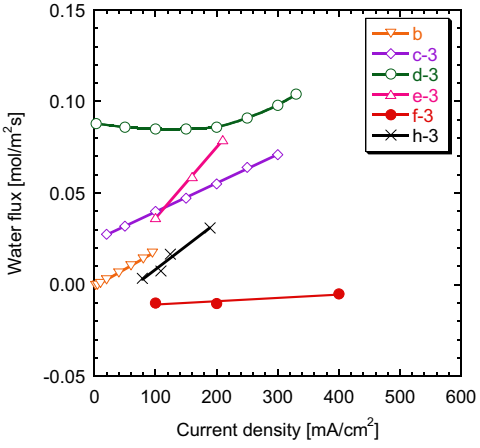

(b) Nafion 117

Fig. 8. Effect of the membrane thickness and the current density on the water flux in different fuel cells.

3.3.3. Comparison of the effect of the fuel concentration on the water transport characteristics between the DFAFC and DMFC

Because the fuel crossover in the DFAFC was lower than that in the DMFC, a higher concentration of formic acid was used in DFAFC than that in the DMFC. For this reason, a quantitative comparison of

Table 4
Slopes and intercepts of the line indicated in Fig. 8.

	Type	Slope ($\times 10^4$)	Intercept ($\times 10^2$)
(a) Nafion 112 (c-1, d-1, e-1, f-1), NRE 211 (g) and NR 212 (h-1)			
c-1	DMFC	1.18	8.74
d-1	DMFC	−0.11	10.77
e-1	DMFC	3.84	−0.18
f-1	PEFC	0.06	−1.43
g	PEFC	−0.05	−0.13
h-1	DFAFC	2.75	−3.24
(b) Nafion 117			
b	DMFC	1.91	−0.11
c-3	DMFC	1.56	2.42
d-3	DMFC	–	(8.24)
e-3	DMFC	3.86	−0.22
f-3	PEFC	0.18	−1.26
h-3	DFAFC	2.56	−1.74

the water transport in the DFAFC and the DMFC is difficult. Therefore, a qualitative comparison of the water transport in the DFAFC and the DMFC was carried out in this section. Based on Figs. 5(b) and 6(b), the total water flux from the anode to the cathode decreased with increasing formic acid concentration irrespective of the membrane thickness. C. Xu et al. reported that the methanol concentration below 4 M had a negligible influence on the water flux through the membrane irrespective of passive operation [20] and active operation [22]. Although a relatively high concentration of fuel was used in the DFAFC, the water flux through the membrane, especially the *y*-intercept, was influenced by the formic acid concentration. This would be related to the hygroscopic property of the formic acid. The hygroscopic properties became strong on increasing the formic acid concentration; therefore, the water flux due to diffusion from the cathode to the anode would be increased with the increasing formic acid concentration. These results indicated that the use of a high concentration of the fuel can contribute to reduction of the water crossover through the membrane, resulting in the reduction of the cathode flooding.

4. Conclusions

The effects of the current density, membrane thickness and formic acid concentration on the water flux through the membrane in the passive DFAFC were investigated to obtain a general understanding of the water transport characteristics. Moreover, the water transport characteristics of the DFAFC were compared with those of the DMFC and PEFC. The passive DFAFCs with insertion of a HF containing different amounts of FEP at the cathode surface were used in this study to measure the water flux over a wide range of current density. By inserting the HF at the cathode surface, the current density was improved irrespective of the membrane thickness, and it increased with the increasing FEP content of the HF in 2 h constant voltage operation. By measuring the water flux during the 2 h operation, it was found that the water crossover through the membrane of the DFAFC linearly increased with increasing current density irrespective of the membrane thickness similar to that in the DMFC; however, it increased with increasing membrane thickness opposite to the DMFC. Moreover, the water flux through the membrane increased with decreasing fuel concentration in the passive DFAFC, although the water crossover in the DMFC was not influenced by the fuel concentration. These differences in the water transport behavior were caused by a difference in the direction of the water flux by diffusion. From these results, it was found that the water transport characteristics in the DFAFC were different from those of the DMFC.

Acknowledgment

A part of this study was supported by JSPS, Grant-in-Aid for Young Scientists (B) (24760628).

References

[1] C. Rice, S. Ha, R.I. Masel, P. Waszczuk, A. Wieckowski, T. Barnard, J. Power Sources 111 (2002) 83–89.
[2] S. Ha, R. Larsen, Y. Zhu, R.I. Masel, Fuel Cells 4 (2004) 337–343.
[3] S. Ha, Z. Dunbar, R. Masel, J. Power Sources 158 (2006) 129–136.
[4] M. Weber, J.T. Wang, S. Wasmus, R.F. Savinell, J. Electrochem. Soc. 143 (1996) L158.
[5] Y.W. Rhee, S.Y. Ha, R.I. Masel, J. Power Sources 117 (2003) 35–38.
[6] X. Wang, J.-M. Hu, I.-M. Hsing, J. Electroanal. Chem. 562 (2004) 73–80.
[7] K.J. Jeong, C.M. Miesse, J.H. Choi, J. Lee, J. Han, S.P. Yoon, S.W. Nam, T.-H. Lim, T.G. Lee, J. Power Sources 168 (2007) 119–125.
[8] W. Dai, H. Wang, X. Yuan, J.J. Martin, D. Yang, J. Qiao, J. Ma, Int. J. Hydrogen Energy 34 (2009) 9461–9478.
[9] T. Colinart, A. Chenu, S. Didierjean, O. Lottin, S. Besse, J. Power Sources 190 (2009) 230–240.
[10] H. Bahrami, A. Faghri, J. Power Sources 230 (2013) 303–320.
[11] Bazylak, Int. J. Hydrogen Energy 34 (2009) 3845–3857.
[12] K. Jiao, X. Li, Prog. Energy Combust. Sci. 37 (2011) 221–291.
[13] M. Ji, Z. Wei, Energies 2 (2009) 1057–1106.
[14] T.S. Zhao, C. Xu, R. Chen, W.W. Yang, Prog. Energy Combust. Sci. 35 (2009) 275–292.
[15] T.S. Zhao, W.W. Yang, R. Chen, Q.X. Wu, J. Power Sources 195 (2010) 3451–3462.
[16] Ismail, S.K. Kamarudin, W.R.W. Daud, S. Masdar, M.R. Yosfiah, J. Power Sources 196 (2011) 9847–9855.
[17] Y. Zhu, S.Y. Ha, R.I. Masel, J. Power Sources 130 (2004) 8–14.
[18] T. Tsujiguchi, S. Hirano, T. Iwakami, N. Nakagawa, J. Power Sources 223 (2013) 42–49.
[19] Y. Zhou, J. Liu, J. Ye, Z. Zou, J. Ye, J. Gu, T. Yu, A. Yang, Electrochim. Acta 55 (2010) 5024–5027.
[20] C. Xu, A. Faghri, X. Li, T. Ward, Int. J. Hydrogen Energy 35 (2010) 1769–1777.
[21] D. Ye, X. Zhu, Q. Liao, J. Li, Q. Fu, J. Power Sources 192 (2009) 502–514.
[22] W.W. Yang, T.S. Zhao, J. Power Sources 188 (2009) 433–446.
[23] C. Xu, T.S. Zhao, J. Power Sources 168 (2007) 143–153.
[24] J.Y. Park, J.H. Lee, S. Kang, J.H. Sauk, I. Song, J. Power Sources 178 (2008) 181–187.
[25] M. Adachi, T. Navessin, Z. Xie, F.H. Li, S. Tanaka, S. Holdcroft, J. Membr. Sci. 364 (2010) 183–193.
[26] S.U. Jeong, E.A. Cho, H.-J. Kim, T.-H. Lim, I.-H. Oh, S.H. Kim, J. Power Sources 159 (2006) 1089–1094.
[27] S. Uhm, S. Chung, J. Lee, J. Power Sources 178 (2008) 34–43.